Investigation into SINS/ANS Integrated Navigation System Based on Unscented Kalman Filtering

Jamshaid Ali*, and Fang Jiancheng**

School of Instrumentation Science and Optoelectronics Engineering,

Beijing University of Aeronautics and Astronautics, Beijing -100083, China

* E-mail: jimmi4u@hotmail.com, Tel: 0086-10-82330104, Fax: 0086-10-82338058

** E-mail: fangjiancheng@buaa.edu.cn , Tel: 0086-10-82316548

Abstract: Strapdown inertial navigation system (SINS) integrated with astronavigation system (ANS) yields reliable mission capability and enhanced navigational accuracy for spacecrafts. The theory and characteristics of integrated system based on unscented Kalman filtering is investigated in this paper. This Kalman filter structure uses unscented transform to approximate the result of applying a specified nonlinear transformation to a given mean and covariance estimate. The filter implementation subsumed here is in a direct feedback mode. Axes misalignment angles of the SINS are observation to the filter. A simple approach for simulation of axes misalignment using stars observation is presented. The SINS error model required for the filtering algorithm is derived in space-stabilized mechanization. Simulation results of the integrated navigation system using a medium accuracy SINS demonstrates the validity of this method on improving the navigation system accuracy with the estimation and compensation for gyros drift, and the position and velocity errors that occur due to the axes misalignments.

Keywords: integrated navigation, SINS, astronavigation, unscented Kalman filter

1. INTRODUCTION

The rationale of the inertial navigation system is the measurement of trajectory of the vehicle in space and the consequent specification of the changes to that trajectory with will bring the vehicle into coincidence with a predetermined target. The trajectories, of course, are functions of the position and velocity vectors of the vehicle. These vectors are usually observed with reference to some reference frame. Powered flight phase of the vehicle is the most decisive phase during which, with the help of navigation information, vehicle is placed on a trajectory with flight conditions which are appropriate for the desired target [1]. Therefore, the navigation accuracy and reliability requirements for an autonomous vehicle necessitate high precision navigation solutions and require the system to provide data unfailingly.

With the swift advancements in the inertial sensor technologies and computing power, SINS has supplanted the conventional gimbaled systems. But, small error sources in the inertial instruments plus capricious variations in the gravitational field forces combine to cause a slow error build up and result is a miss distance at the target. The extended duration of the vehicle's flight and absence of updates from the ground sources lead to a greater probability of errors in the navigation solution. Therefore, an external aiding is deemed vital to augment the navigation system for precision guidance. The Global Positioning System (GPS) is a prevalent choice for SINS augmentation but its vulnerability to jamming and degraded accuracy in hostile environments makes it an indigent option. The astronavigation system, as has been used in the past, is still popular and finds its application in the modern space missions. Consequently, SINS integrated with ANS using a nonlinear filtering technique is the subject of this paper.

For short and medium range guided munitions, gyro drift has a significant contribution to navigation error. ANS is an effective source to estimate in-flight gyros drift and also the velocity and position errors contributed by the drift. As an alternate to the more conventional GPS, which is vulnerable to jamming and other disturbances, ANS cannot be disturbed as easily, and the system is impossible to jam. As its intended use is with spacecrafts, this system works in space where there is no hindrance in star observation. In this way, it is all weather and all time navigation aid. With the technological progress and image processing techniques, ANS has become camera based navigation system where charge coupled device (CCD) array, mounted in strapdown configuration, is used as a star sensor. Current CCD sensors provide a relatively inexpensive way to image sky and extract the required information. Body fixed sensors can scan a section of the sky and determine the association between the scanned stars and the catalog of reference stars stored onboard using some star identification techniques. Stars identification leads to estimate attitude information.

The mainstay to an integrated navigation system is the concept of fusing noisy observations from SINS and ANS for an enhanced navigation solution. Kalman filter, an optimal recursive dada processing algorithm, has been widely used in the integrated navigation systems. The Kalman filter processes all available measurements of a variable of interest, regardless of their accuracy, based on the knowledge of the system and measurement dynamics, the statistical description of the system noises, and model uncertainties [2]. In some cases the model may be linear, but most systems models are nonlinear in nature. In this paper, we apply the unscented Kalman filter (UKF) framework to the problem of nonlinear estimation and sensor fusion for the SINS/ANS integration. The fundamental component of this filter is the unscented transformation which uses a set of approximately chosen weighted points to parameterize the means and covariances of probability distributions [9].

This paper is systematized in 6 sections. In section 2, SINS error models are presented with definitions of the frames of reference used. Error models are derived for space-stabilized mechanization. Integrated navigation system configuration is presented and the system dynamic and measurement models are elaborated in section 3. This section also presents an algorithm for estimation of SINS axes misalignment angles. Section 4 deals with the UKF algorithm for integration and its implementation remuneration. Simulation is carried out for the ballistic missile application and powered phase trajectory data is used. The correction of velocity errors induced by attitude errors is mentioned. Simulation minutiae and results are presented in section 5. This paper is concluded in section 6.

2. SINS ERROR MODEL

2.1 Coordinate Frames

Coordinate frames used in this paper are defined as follows [3]

- a. Inertial frame (i-frame)
- b. Navigation frame (n-frame)
- c. Launch inertial frame (il-frame)
- d. Body frame (b-frame)
- e. Observed star frame (j-frame)

The i-frame has its origin at earth center with z-axis normal to the equatorial plane, x-axis in equatorial plan and y-axis complements the right handed system. The n-frame is a local level frame with z-axis parallel to the upward vertical, x-axis points eastward and y-axis points northward. The il-frame has its origin at the launch point. It is a local level frame (i.e. x and y axes form a level plane) while y-axis aims towards the expected target. In b-frame of the vehicle, x-axis is along longitudinal axis, z-axis is perpendicular to longitudinal plan of symmetry and y-axis complements the right handed system. We assume a j-frame for the jth observed star that has been identified as guide star in the reference star catalog. Figure 1 depicts the relationship between i and j frame. The angles Θ_j and Γ_j represent jth star's right ascension and declination respectively.
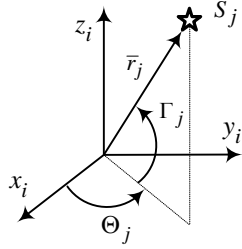
Fig. 1 Inertial and star frame

2.2 Attitude Error Model

In this paper, space-stabilized mechanization is used for the SINS. It is conceptually the simplest of all possible system implementations, since Newton's laws are most simply stated in an inertial frame of reference. The space-stabilized inertial navigation system outputs navigation parameters in an inertially non-rotating frame [4]. Thus, this mechanization is free of Earth's rotation and transport rate. In this perspective, attitude error can simply be articulated as

$$\dot{\bar{\phi}} = C_b^{il}(\bar{\varepsilon}^b + \bar{w}^b) \tag{1}$$

where ϕ represents SINS axes misalignment error or attitude error; C_b^{il} is transformation matrix between indicated frames; ε and w denote gyros constant and random drifts respectively. Equation (1) can also be written as

$$\begin{bmatrix} \dot{\phi}_x \\ \dot{\phi}_y \\ \dot{\phi}_z \end{bmatrix} = \begin{bmatrix} c_{11} & c_{12} & c_{13} \\ c_{21} & c_{22} & c_{23} \\ c_{31} & c_{32} & c_{33} \end{bmatrix} \begin{bmatrix} \varepsilon_x^b + w_x^b \\ \varepsilon_y^b + w_x^b \\ \varepsilon_z^b + w_x^b \end{bmatrix} \tag{2}$$

2.3 Velocity and Position Error Model

Velocity error equation in the space-stabilized mechanization is given as

$$\delta\dot{\bar{v}}^{il} = \bar{f}^{il} \times \bar{\phi}^{il} + C_b^{il}(\bar{\nabla}^b + \bar{\upsilon}^b) + \delta\bar{g}^{il} \tag{3}$$

where f is the specific force measured by accelerometers; δg is the acceleration error due to gravity; ∇ and υ represent accelerometer constant and random bias respectively.

In this paper, ellipsoidal Earth model is assumed for which gravity vector in the reference navigation frame is expressed as [4]

$$\bar{g}^{il} = -C_i^{il} \frac{\mu}{r^3} \begin{bmatrix} \{1 + \frac{3}{2}J_2(r_e/r)^2[1 - 5(r_z^i/r)^2]\}r_x^i \\ \{1 + \frac{3}{2}J_2(r_e/r)^2[1 - 5(r_z^i/r)^2]\}r_y^i \\ \{1 + \frac{3}{2}J_2(r_e/r)^2[3 - 5(r_z^i/r)^2]\}r_z^i \end{bmatrix} \tag{4}$$

where μ = product of the Earth's mass and universal gravitational constant = $(3.9860305 \pm 3 \times 10^{-7}) \times 10^{14} [m^3/s^2]$

r = geocentric position vector magnitude = $\sqrt{r_x^{i2} + r_y^{i2} + r_z^{i2}}$

J_2 = a constant coefficient = $(1.08230 \pm 0.0002) \times 10^{-3}$

r_e = the Earth's equatorial radius = 6378137[m]

r_x^i, r_y^i, r_z^i = components of geocentric position vector

C_i^{il} is the transformation matrix between indicated frames

Hence, acceleration error due to gravity can be expressed as

$$\delta\bar{g}^{il} = C_i^{il} \begin{bmatrix} \partial g_x^i/\partial r_x^i & \partial g_x^i/\partial r_y^i & \partial g_x^i/\partial r_z^i \\ \partial g_y^i/\partial r_x^i & \partial g_y^i/\partial r_y^i & \partial g_y^i/\partial r_z^i \\ \partial g_z^i/\partial r_x^i & \partial g_z^i/\partial r_y^i & \partial g_z^i/\partial r_z^i \end{bmatrix} \tag{5}$$

Position error equation in rectangular coordinates is given as

$$\delta\dot{\bar{r}}^{il} = \delta\bar{v}^{il} \tag{6}$$

3. INTEGRATED NAVIGATION SYSTEM

3.1. Configuration

The configuration of integrated system is depicted in Fig. 2. Here, stars observations are made by CCD star sensors, generating a two dimensional image of a small section of the sky. The image output from the camera goes to the onboard computer. Computer programs, through some video thresholding schemes, limit the number of stars in a field that will be processed. Stored in the computer memory is a star catalog with the celestial coordinates of each star, in some reference system, which will be used for star field recognition through some image matching techniques [3].

To trim down cost and size, and to improve consistency, an advanced configuration utilizes a star sensor rigidly mounted on the strapdown IMU. This arrangement has become viable through technology advances and computing power. In this case, image is not stabilized on the focal plane; rather, it is computationally stabilized. The fully strapdown configuration requires the use of a very wide FOV telescope. The size of the focal plane array must be coherent with the FOV requirements. The contents of onboard star catalog are significantly increased as compared to platform configuration. In this system, the best configuration is to use two star sensors and associated electronics with a dedicated microprocessor [5].
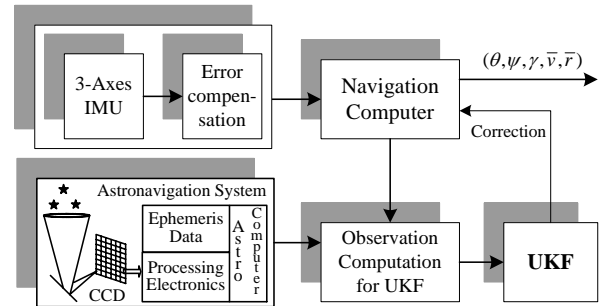
Fig. 2 SINS/ANS integrated navigation system

3.2 SINS Axes Misalignment Angles

Suppose $\bar{r}_j^{\,j}$ represents unit position vector of the jth star projected into j-frame, then its transformation into i-frame using star's right ascension and declination yields

$$\bar{r}_j^{\,i} = C_j^i \bar{r}_j^{\,j} \tag{7}$$

From the image projection geometry on two dimensional plane as shown in Fig. 3, we get star's bearing and elevation angles in the star sensor frame.
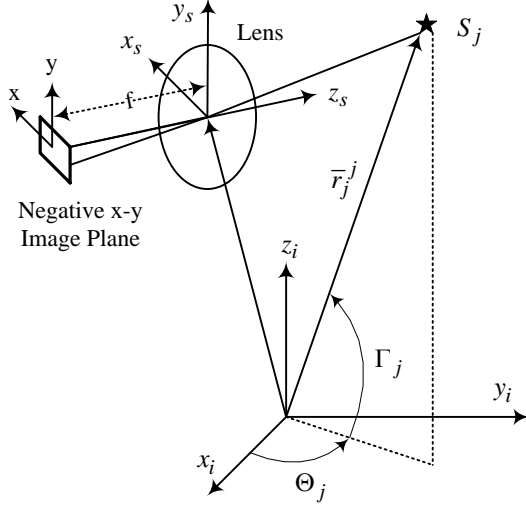

Fig. 3 Star's projection geometry

As we know the orientation of the sensor with respect to body frame, we get jth star unit position vector in body frame as

$$\bar{r}_j^{\,b} = C_s^b C_j^s \bar{r}_j^{\,j} \tag{8}$$

Estimated star's position vector in the navigation frame is

$$\hat{\bar{r}}_j^{\,il} = \bar{r}_j^{\,p} = C_b^p \bar{r}_j^{\,b} \tag{9}$$

where p represents mathematical platform frame and C_b^p is the estimated attitude matrix from SINS.

For small angle approximations, the relationship between the mathematical platform frame and the reference navigation frame is as follows

$$C_{il}^p = \begin{bmatrix} 1 & \phi_z & -\phi_y \\ -\phi_z & 1 & \phi_x \\ \phi_y & -\phi_x & 1 \end{bmatrix} = I - \Phi \tag{10}$$

Unit position vector of the jth star in p frame can also be expressed as

$$\bar{r}_j^{\,p} = C_i^p \bar{r}_j^{\,i} = (I - \Phi)\bar{r}_j^{\,i} \tag{11}$$

If there are n number of stars in the FOV of the star sensor, Eqs. (9) and (11) can be equated to get the following relationship

$$\begin{bmatrix} \bar{r}_1^{\,p} & \bar{r}_2^{\,p} & . & . & . & \bar{r}_n^{\,p} \end{bmatrix} = (I - \Phi)\begin{bmatrix} \bar{r}_1^{\,i} & \bar{r}_2^{\,i} & . & . & . & \bar{r}_n^{\,i} \end{bmatrix} \tag{12}$$

In simplified form Eq. (12) can be written as

$$R_p = (I - \Phi)R_i \tag{13}$$

where $R_p = \begin{bmatrix} \bar{r}_1^{\,p} & \bar{r}_2^{\,p} & \bar{r}_3^{\,p} & . & . & \bar{r}_N^{\,p} \end{bmatrix}$ and

$$R_i = \begin{bmatrix} \bar{r}_1^{\,i} & \bar{r}_2^{\,i} & \bar{r}_3^{\,i} & . & . & \bar{r}_N^{\,i} \end{bmatrix}$$

From Eq. (13) we get axes misalignment matrix as

$$\hat{\Phi} = I - R_p R_i^T (R_i R_i^T)^{-1} \tag{14}$$

3.3 Dynamical and Measurement Model of the System

The nonlinear system's dynamic and observation equations for the Kalman filter in discrete form are given as [6]

$$\begin{aligned} x_k &= f(x_{k-1}, k-1) + G_{k-1}w_{k-1}, \quad k = 0,1,.., \\ z_k &= h_k(x_k) + \vartheta_k \end{aligned} \tag{15}$$

where $f_k() \in \mathbb{R}^{n \times n}$ is the process model; $x_k \in \mathbb{R}^n$ is the state vector; G_k is the system noise matrix; $w_k \in \mathbb{R}^n$ is the system noise; $z_k \in \mathbb{R}^p$ is the measurement vector; $h_k() \in \mathbb{R}^{p \times n}$ is the measurement model and $\vartheta_k \in \mathbb{R}^p$ is the measurement noise. We assume that noise is uncorrelated Gaussian white noise sequences with mean and covariances as follows:

$$E\{w_i\} = 0; \quad E\{w_i w_j\} = Q\delta_{ij}$$
$$E\{\vartheta_i\} = 0; \quad E\{\vartheta_i \vartheta_j\} = R\delta_{ij}$$
$$E\{w_i \vartheta_j\} = 0 \text{, for all } i, j$$

where $E\{\cdot\}$ denotes the expectation, and δ_{ij} is the Kronecker delta function.

Q and R are bounded positive definite matrices (Q>0, R>0). Initial state x_0 is normally distributed with zero mean and covariance P_0.

In our system, dynamical model of the system is defined by the error differential Eqs. (2), (3) and (6). System's transition matrix and the system and measurement noise covariance matrices are transformed to discrete form for implementation. System state vector used is as below

$$x_k = \begin{bmatrix} \phi_x, \phi_y, \phi_z, \delta v_x, \delta v_y, \delta v_z, r_x, r_y, r_z, \varepsilon_x, \varepsilon_y, \varepsilon_z, \nabla_x, \nabla_y, \nabla_z \end{bmatrix}^T$$

Input noise matrix is

$$G_k = [I_{6\times6}; 0_{9\times6}] \text{, where I is the identity matrix}$$

The measurement vector is expressed as

$$z_k = [\phi_x + \sigma_x \quad \phi_y + \sigma_y \quad \phi_z + \sigma_z]^T$$

where $(\sigma_x, \sigma_y, \sigma_z)$ represent attitude errors contribution from the astronavigation system.

4. UNSCENTED FILTERING ALGORITHM

4.1 The Choice of UKF

The fundamental and imperative operation performed in all Kalman filters is the propagation of the Gaussian random variables through the system dynamics. For the nonlinear system applications, in the extended Kalman filter (EKF), the system state distribution and all relevant noise densities are approximated by these random variables, which are then propagated analytically through the first order linearization of the nonlinear system. This can lead into large errors in the true posterior mean and covariance of the transformed random variable, which may yield suboptimal performance and sometimes divergence of the filter. The UKF embarks upon this problem by using a deterministic sampling methodology. The state distribution is again approximated by a random variable but represented using minimal set of carefully chosen weighted sample points. These sample points completely capture the true mean and covariance of random variable, and when propagated through the true nonlinear system, captures the posterior mean and covariance for any nonlinearity. The EKF, on the contrary, only achieves the first order accuracy. Remarkably, the computational complexity of the UKF is the same order as that of EKF. What's more, realization of the UKF is often considerably easier and requires no analytic

derivation or Jacobians as in the EKF. The UKF methods has demonstrated to be far superior to standard EKF based estimation approaches in a wide range of applications in the areas of nonlinear state estimation [7,8].

4.2 The UKF Implementation Equations

Following steps are followed for implementation of the UKF in the integrated navigation system [7-10]:

a. Find weights for the states and covariance matrices as

$$
\left.\begin{aligned}
W_0^s &= \lambda/(n_s + \lambda) \\
W_0^c &= (1 - \alpha^2 + \beta) + 0.5\lambda/(n_s + \lambda) \\
W_i^s &= W_i^c = 0.5\lambda/(n_s + \lambda), \quad i = 1, \cdots, 2n_s
\end{aligned}\right\} \quad (16)
$$

where:

n_s is the number of the states in the augmented state vector

λ is a scaling parameter $= \alpha^2(n_s + \kappa) - n_s$, where α determines how the sigma points are spread, typical value is 10^{-3}; κ is a scaling parameter which can be used to incorporate up to fourth order precision in the transformation, usually set to zero. β is used to incorporate knowledge of the distribution of states, optimal value for Gaussian distribution is 2; s and c in the subscript and superscript denote state and covariance respectively.

b. Create a set of sigma points $\chi_{i,k-1}$ with $\hat{x}_{k-1}$ and P_{k-1}, using following set of equations

$$
\left.\begin{aligned}
\chi_{0,k-1} &= \hat{x}_{k-1}, \\
\chi_{i,k-1} &= \hat{x}_{k-1} + (\sqrt{(n_s + \lambda)P_{k-1}})_i, i = 1, \cdots, n_s \\
\chi_{i,k-1} &= \hat{x}_{k-1} - (\sqrt{(n_s + \lambda)P_{k-1}})_i, i = n_s + 1, \cdots, 2n_s
\end{aligned}\right\} \quad (17)
$$

where:

χ is the sigma points of the augmented state vector,

P_{k-1} is the old prediction of the covariance

c. Prediction: The sigma points are then propagated through the nonlinear system and measurement models as

$$
\left.\begin{aligned}
\chi_{k,k-1} &= f(\chi_{k-1}, k-1) \\
Z_{k,k-1} &= h(\chi_{k-1})
\end{aligned}\right\} \quad (18)
$$

The prediction of the state and measurement vector as well covariance of the state vector is performed as

$$
\left.\begin{aligned}
\hat{x}_k^- &= \sum_{i=0}^{2n_s} W_i^s \chi_{i,k|k-1}, \quad \hat{z}_k = \sum_{i=0}^{2n_s} W_i^m Z_{i,k|k-1} \\
P_k^- &= \sum_{i=0}^{2n_s} W_i^c (\chi_{i,k|k-1} - \hat{x}_k^-)(\chi_{i,k|k-1} - \hat{x}_k^-)^T + Q
\end{aligned}\right\} \quad (19)
$$

d. Update: Update the measurement prediction covariance, the cross covariance between the state and measurement, the Kalman gain, the state estimate and the state covariance as

$$
\left.\begin{aligned}
P_{\hat{z}_k \hat{z}_k} &= \sum_{i=0}^{2n_s} W_i^c (Z_{i,k|k-1} - \hat{z}_k)(Z_{i,k|k-1} - \hat{z}_k)^T + R \\
P_{\hat{x}_k \hat{z}_k}^- &= \sum_{i=0}^{2n_s} W_i^c (\chi_{i,k|k-1} - \hat{x}_k^-)(Z_{i,k|k-1} - \hat{z}_k)^T
\end{aligned}\right\} \quad (20)
$$

$$
\left.\begin{aligned}
K_k &= P_{\hat{x}_k \hat{z}_k} P_{\hat{z}_k \hat{z}_k}^{-1} \\
\hat{x}_k^+ &= \hat{x}_k^- + K_k(z_k - \hat{z}_k) \\
\hat{P}_k^+ &= P_k^- - K_k P_{\hat{z}_k \hat{z}_k} K_k^T
\end{aligned}\right\} \quad (21)
$$

e. The processing for the current epoch is completed. Return to step b to process for the next epoch.

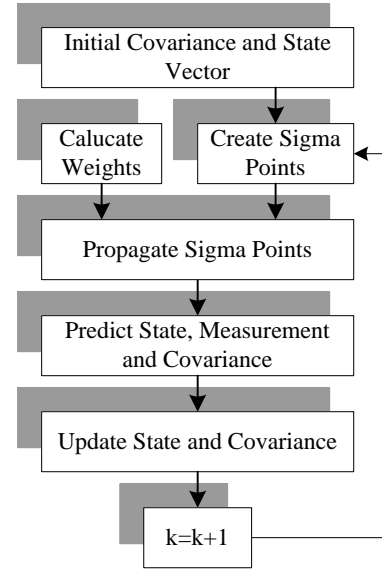The block diagram of the UKF implementation algorithm is shown in Fig. 4.

Fig. 4 The UKF algorithm

5. SIMULATION AND RESULTS

The discrete UKF realization used in this paper is the direct feedback where the estimated errors are fed back to the SINS, thus minimizing the evolution of the observed errors those are to be delivered as an observation to the Kalman filter [2]. In this simulation, quaternion is obtained from the corrected attitude matrix and is fed back for attitude error compensation.

Parameters of a medium accuracy SINS are used for initialization of the UKF. ANS augmentation comes into effective 40 seconds after lift off of the missile when it attains altitude above 22 km from onwards stars are visible unhindered [11]. SINS computations are carried out at 80 Hz while ANS aiding is provided at 1 Hz. Simulation is carried out for the powered flight trajectory of the ballistic missile as shown in Fig. 5.
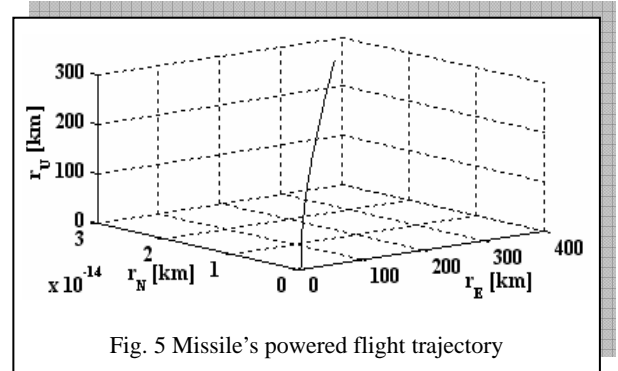

Fig. 5 Missile's powered flight trajectory

The results for the UKF estimated axes misalignment angles and the gyros drifts are shown in Figs. 6 and 7 respectively.

In the SINS/ANS integrated navigation system, observability of the velocity and position errors is poor. From the simulation, we estimate axes misalignment angles and the constant gyros drifts. The drift represents gyro turn-on to turn-on constant drift which is estimated using ANS aiding. Thus, from the observable attitude errors states, we can estimates and compensate for the velocity as well as position errors that occur due to the axes misalignments. This

compensation takes place when the vehicle is out of atmosphere and the astronavigation comes into effect. The velocity errors caused by axes misalignment angles before and after the ANS aiding are shown in Fig. 8.

6. CONCLUSIONS

Astronavigation aiding for SINS is an attractive solution for in-flight estimation and compensation of navigation errors arising from gyros drift. In this paper, for reliable targeting of guided munitions, an accurate modeling of the Earth's gravitational filed is employed that is nonlinear in nature. The UKF implementation solves this nonlinear state estimation problem in an elegant way without approximations loss.
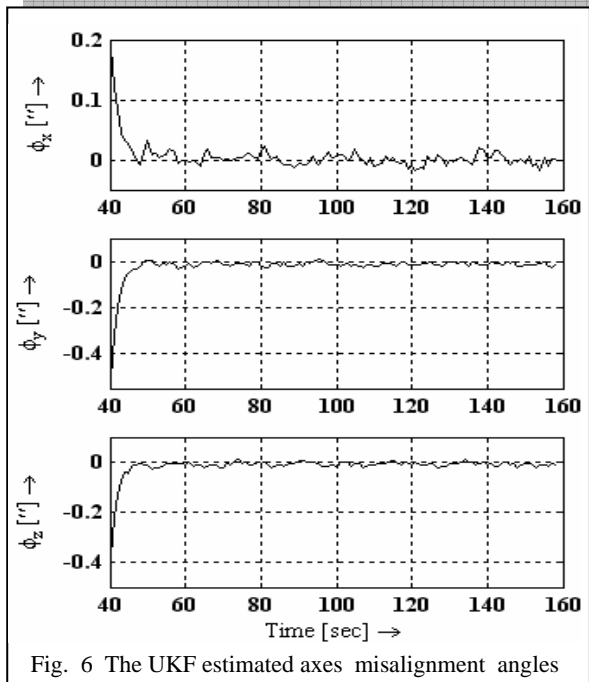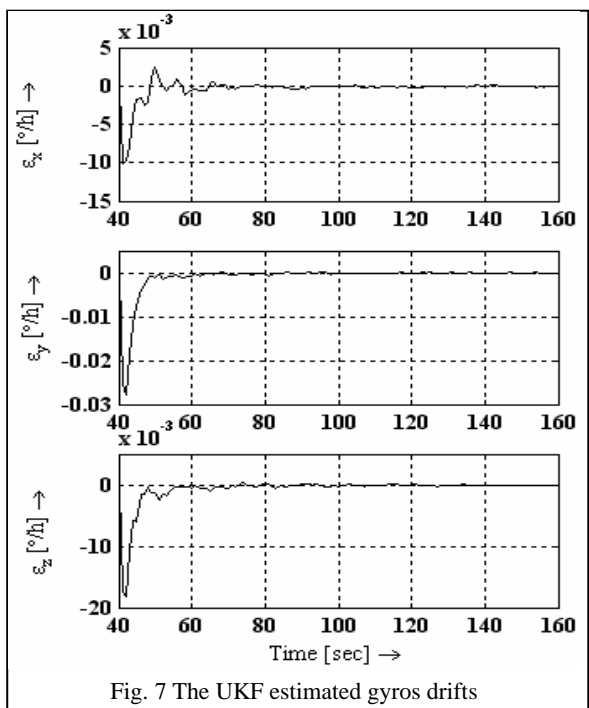
Fig. 6 The UKF estimated axes misalignment angles

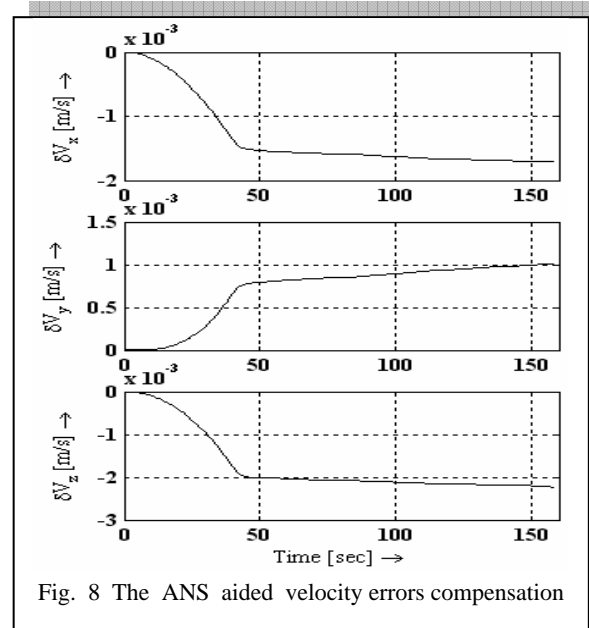Fig. 7 The UKF estimated gyros drifts

Fig. 8 The ANS aided velocity errors compensation

REFERENCES

[1] E. V. B. Stearns, "Navigation and Guidance in Space," Prentice-Hall, Inc., 1963.

[2] P. S. Maybeck, "Stochastic Models, Estimation and Control," Academic Press, 1982.

[3] J. Ali, and J. C. Fang, "In-flight Alignment of Inertial Navigation System using Celestial Observation Technique," In Proc. of the International Symposium on Inertial Navigation Technology and Intelligent Traffic, Nanjing, China, 2004.

[4] K. R. Britting, "Inertial Navigation Systems Analysis," Wiley-Interscience, 1971.

[5] M. Kayton and W. R. Fried, Avionics Navigation Systems, John Wiley and Sons, Inc. 1997.

[6] A. Romanenko and J. A. Castro, "The Unscented Filter as an Alternative to the EKF for Nonlinear State Estimation: A Simulation Case Study," Computers and Chemical Engineering 28, 2004, pp. 347-355.

[7] S. J. Julier, and J. K. Uhlmann, "Unscented Filtering and Nonlinear Estimation," In Proc. of the IEEE, Vol. 92, No. 3, pp. 401~422, 2004.

[8] R. van der Merwe and E. Wan, "Sigma Point Kalman Filters for Integrated Navigation," In Proc. of the 60th Annual Meeting of the Institute of Navigation, Dayton, OH, June, 2004.

[9] S. J. Julier, and J. K. Uhlmann, "A New Extension of the Kalman Filter to Nonlinear Systems," In Proc. of AeroScene: the 11th International Symposium on Aerospace/Defense Sensing, Simulation and Control, Orlando, USA, 1997, pp. 182-193.

[10] S. J. Julier, and J. K. Uhlmann, "A New Approach for Filtering Nonlinear Systems," In Proc. of the American Control Conference, 1995, pp. 1628-1632.

[11] S. Levine, "AGARDograph on Advanced Astroinertial Navigation Systems," AGARD-AG-331, Aerospace Navigation Systems, 1995, pp. 187-199.

[12] J. Ali and C. Y. Zhang, "Simulation Algorithm for SINS Axes Misalignment Angles through Stars Observation," In Proc. of the 11th Saint Petersburg International Conference on Integrated Navigation Systems, Russia, 2004, pp. 129-130.